



1 **The higher relative concentration of K^+ to Na^+ in saline**
2 **water improves soil hydraulic conductivity, salt leaching**
3 **efficiency and structural stability**

4 Sihui Yan ^{a,b}, Binbin Zhang ^{a,b}, Tonggang Zhang ^{a,b}, Yu Cheng ^{a,b}, Chun Wang ^{a,b}, Min

5 Luo ^{a,b}, Hao Feng ^{a,c}, Tibin Zhang ^{a,c,*}, Kadambot H.M. Siddique ^d

6 ^a. Key Laboratory of Agricultural Soil and Water Engineering in Arid and Semiarid

7 Areas, Ministry of Education, Northwest A&F University, Yangling, Shaanxi 712100,

8 P. R. China

9 ^b. College of Water Resources and Architecture Engineering, Northwest A&F

10 University, Yangling, Shaanxi 712100, P. R. China

11 ^c. Institute of Soil and Water Conservation, Northwest A&F University, Yangling,

12 Shaanxi 712100, P. R. China

13 ^d The UWA Institute of Agriculture, The University of Western Australia, Perth, WA

14 6001, Australia

15 * Corresponding author at: Institute of Soil and Water Conservation, Northwest A&F

16 University, Yangling, Shaanxi 712100, China. Tel.: +86 29 87012871; fax: +86 29

17 87011354. E-mail: zhangtubin@163.com (T. Zhang)



18 Abstract

19 Soil salinity and sodicity caused by saline water irrigation are widely observed
20 globally. Clay dispersion and swelling are influenced by sodium (Na^+) concentration
21 and electrical conductivity (EC) of soil solution. Specifically, soil potassium (K^+) also
22 significantly affects soil structural stability, but which concern was rarely addressed in
23 previous studies or irrigation practices. A soil column experiment was carried out to
24 examine the effects of saline water with different relative concentrations of K^+ to Na^+ ,
25 including K^+/Na^+ of 0:1 (K0Na1), 1:1 (K1Na1), 1:0 (K1Na0) at a constant EC (4 dS m^{-1}),
26 and deionized water as the control (CK), on soil physicochemical properties. The
27 results indicated that at the constant EC of 4 dS m^{-1} , the infiltration rate and water
28 content were significantly ($P < 0.05$) affected by K^+/Na^+ values, K0Na1, K1Na1 and
29 K1Na0 significantly ($P < 0.05$) reduced saturated hydraulic conductivity by 43.62%,
30 29.04% and 18.06% respectively compared with CK. The volumetric water content was
31 significantly ($P < 0.05$) higher in K0Na1 than CK at both 15 and 30 cm soil depths.
32 K1Na1 and K1Na0 significantly ($P < 0.05$) reduced the desalination time and required
33 leaching volume. K0Na1 and K1Na1 reached the desalination standard after the fifth
34 and second infiltration, respectively, as K1Na0 did not exceed the bulk electrical
35 conductivity required for desalination prerequisite throughout the whole infiltration
36 cycle at 15 cm soil layer. Furthermore, due to the transformation of macropores into
37 micropores spurred by clay dispersion, soil total porosity in K0Na1 dramatically
38 decreased compared with CK, and K1Na0 even increased the proportion of soil



39 macropores. The higher relative concentration of K^+ to Na^+ in applied water was more
40 conducive to soil aggregates stability, alleviating the risk of macropores reduction
41 caused by sodicity.

42 **Keywords:** Saline water; Cation composition; Hydraulic properties; Desalination; Pore
43 structure.

44 **1 Introduction**

45 Freshwater shortage resulted from elevated demand for water resources as well as
46 the irrational exploitation and use after economic and population growth (Zhang and
47 Xie 2019; Prajapati et al. 2021), constrains the sustainability of agricultural production
48 (Aparicio et al., 2019). Alternative water resources with variable water quality (such as
49 saline water) are being considered for agricultural irrigation in several desert and saline
50 areas (Singh et al. 2021; Liu et al. 2022a). Utilizing saline water could partly alleviate
51 the undersupply of freshwater for agricultural production (Yang et al., 2020). However,
52 the other side of the coin is that saline water irrigation could result in soil salinization
53 and/or sodicity. This disaster is related directly to soil pore size distribution, and in turn
54 to the dispersion and swelling of the clay fraction (Bouksila et al. 2013; Hack-ten
55 Broeke et al. 2016; Zhang et al. 2018). Therefore, in order to optimize saline water
56 utilization, the effects of saline water quality on the soil hydraulic properties and pore
57 structure characteristics should be paid more attention (Scudiero et al., 2017).

58 Saline water irrigation can increase the monovalent ions concentration in soil



59 solution and affect soil structure (Qadir et al. 2007; Qadir et al. 2021). Excess sodium
60 (Na^+) from irrigation saline water is adsorbed onto the clay exchange surface in salt-
61 affected soils where sodium compounds predominate contributing to the disintegration
62 of soil structure (Marchuk and Rengasamy 2011; Belkheiri and Mulas 2013; Awedat et
63 al. 2021). As percolation progresses, the thickness of the diffusion double electron
64 layers raises due to the relatively larger hydrated radius of Na^+ , and the repulsive force
65 between adjacent diffusion double electron layers appears to increase, resulting in the
66 dispersion and swelling of soil particles (Alva et al. 1991; Reading et al. 2015).

67 Soil calcium (Ca^{2+}) and magnesium (Mg^{2+}) can alleviate soil dispersibility by
68 replacing Na^+ in soil colloids, the outer layer of the Ca^{2+} and Mg^{2+} containing colloidal
69 particles do not adsorb water molecules, turning Na^+ qualitative hydrophilic colloid into
70 Ca^{2+} and Mg^{2+} hydrophobic colloid (Marchuk and Rengasamy 2011; Tsai et al. 2012).
71 Colloidal particles get close to each other, promoting soil particles forming water stable
72 aggregates, thus improving soil structural stability (Gharaibeh et al. 2009; McKenna et
73 al. 2019). Therefore, the concentration of Na^+ in relation to Mg^{2+} and Ca^{2+} (Sodium
74 adsorption ratio, SAR) (U.S. Salinity Laboratory Staff 1954) is considered a crucial
75 criterion in soil structural stability and hydraulic conductivity (Rengasamy and
76 Marchuk 2011). Although SAR can be used to predict soil clay dispersion effect caused
77 by cations, the controlling mechanism of dispersion in SAR is presumed to be
78 exchangeable Na^+ . However, Na^+ does not alone cause soil dispersion since the
79 chemical component of clay structure integrity is mainly a function of ionic valence



80 and hydration radius (Marchuk et al., 2014). Potassium (K^+) has been overlooked
81 because salt-affected soils typically contain low amounts of K^+ . However, Li et al.
82 (2022) reported that under the continuous recycling use of underground saline water,
83 water-soluble and exchangeable K^+ is higher than Ca^{2+} and Mg^{2+} in the Hetao irrigation
84 district—one of the large irrigation districts in China. It is anticipated that the long-term
85 use of irrigation water with high K^+ concentrations may therefore create substantial
86 challenges in preserving good soil structure and adequate infiltration rates (Sposito et
87 al., 2016). K^+ is not as effective as Na^+ in generating soil particle dispersion and
88 swelling problems, yet Marchuk and Marchuk (2018) pointed out that K^+ could
89 substitute Na^+ on exchange sites to encourage Na^+ leaching and increase water
90 conductivity to some extent. A lower concentration of K^+ may have positive effects on
91 soil permeability due to the substitution of exchangeable Na^+ by K^+ with lower
92 dispersive potential, increasing aggregates stability and soil pore connectivity (Buelow
93 et al., 2015).

94 Thus, we hypothesized that the amount of K^+ relative to Na^+ would certainly have
95 an effect on soil structural stability, and these relationships could be well evaluated by
96 a column experiment under controlled conditions. The specific objectives of this study
97 were to (1) ascertain the effect of irrigation saline water with different relative
98 concentrations of K^+ to Na^+ (K^+/Na^+) on transport and distribution of water and salt; (2)
99 determine the effect on soil pore structural characteristics; (3) predict these effects using
100 a newly proposed index (CROSS) rather than SAR.



101 **2 Materials and methods**

102 **2.1 Soil sampling location and properties**

103 The study soil was collected from a layer of 0-40 cm field in Yangling (108°04'E,
104 34°20'N), Shaanxi Province, China. After air-dried, the soil was grounded to pass
105 through a 2-mm sieve. Soil physical and chemical properties are listed in Table 1. Soil
106 particle size distribution was measured by the Laser Mastersizer 2000 (Malvern
107 Instruments, Malvern, UK), and according to the USDA classification system, soil
108 texture is classified as silty clay loam. Soil bulk density calculated by soil core method
109 was 1.35 g cm⁻³. The soil had a low salt concentration with EC_e (electrical conductivity
110 of saturated extract) of 0.72 dS m⁻¹ and pH of 7.66, respectively. EC_e and pH were
111 measured by conductivity meter (DDS-307, China) and pH meter (PHS-3C, China),
112 respectively. Flame photometry (6400A, China) was used to measure soluble Na⁺ and
113 K⁺, CO₃²⁻ and HCO₃⁻ concentrations were tested by the neutral titration method, Cl⁻ was
114 analyzed by the silver nitrate titration method, and SO₄²⁻ was determined by barium
115 sulfate turbidimetric method, Mg²⁺ and Ca²⁺ were specified using ethylene diamine
116 tetraacetic acid (EDTA) titrimetric method (Bao 2005).

117

118

119

120



121 Table 1 The physicochemical properties of study soil.

Property	Value
Particle size distribution (%)	
Sand (> 0.05 mm)	8.10
Silt (0.05-0.002 mm)	60.62
Clay (<0.002 mm)	31.28
Texture	Silty clay loam
EC _e (dS m ⁻¹)	0.72
pH	7.66
Ion concentration (mmol L ⁻¹)	
CO ₃ ²⁻ +HCO ₃ ⁻	0.60
Cl ⁻	0.23
SO ₄ ²⁻	2.18
Mg ²⁺	0.32
Ca ²⁺	0.54
Na ⁺	0.10
K ⁺	< 0.01

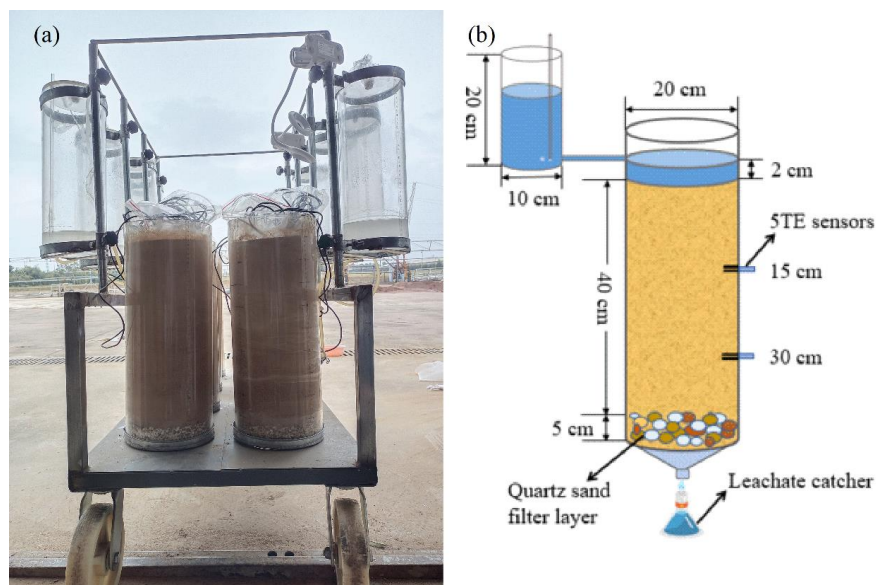
122 Note: EC_e represents electrical conductivity of soil saturated extract.

123 2.2 Experiment design

124 Soil columns were prepared using transparent polyvinyl chloride cylinders, with
125 an internal diameter of 20 cm and a height of 50 cm (Fig. 1). Round and small holes (6
126 mm diameter) were equally arranged at the bottom for drainage. A 5 cm depth quartz
127 sand was laid at the bottom of the soil column as a filter layer before packing to prevent
128 small soil particles from being washed away. After that, air-dried soil was packed at 40
129 cm height with a bulk density of 1.35 g cm⁻³ (referring to the original level of the soil).
130 The sieved dry soil was poured into each soil column in the 5-cm sections for uniform
131 compaction, and the layer's surface was roughened to ensure a tight connection to the
132 next layer. The soil column was then allowed to stand in the laboratory for 24 hours



133 before the initiation of the experiments described herein. The constant water head (2
134 cm, using a Mariotte bottle) infiltration experiment was conducted with three
135 replications for each treatment.



136
137 Fig. 1. Illustration of the experiment apparatus (a) and schematic diagram (b).

138 Three infiltration solutions were prepared with different ratios of K^+/Na^+ (0:1
139 (K0Na1), 1:1 (K1Na1), 1:0 (K1Na0) at constant EC of 4 dS m^{-1} and deionized water as
140 the control (CK) (Table 2). The cation ratio of soil structural stability (CROSS)
141 (Rengasamy and Marchuk 2011) was an indicator of soil structural behavior as
142 influenced by both Na^+ and K^+ , and it was calculated accordingly (Smith et al., 2015):

143

$$CROSS = \frac{Na^+ + 0.335K^+}{\left[(Ca^{2+} + 0.0758Mg^{2+}) / 2 \right]^{0.5}} \quad (1)$$

144 where different chemical element symbols denote charge concentrations ($\text{mmol}_c \text{ L}^{-1}$).

145



146 Table 2 Saline water settings with different K^+/Na^+ at a constant EC.

Treatment	Adding salt/ (mmol L ⁻¹)			K^+/Na^+	Setting	Measured	CROSS
	KCl	NaCl	CaCl ₂		EC	EC	
					(dS m ⁻¹)	(dS m ⁻¹)	(mmol _c L ⁻¹) ^{0.5}
K0Na1	0	34	3	0:1	4.00	4.25	27.76
K1Na1	17	17	3	1:1	4.00	4.33	17.49
K1Na0	34	0	3	1:0	4.00	4.40	7.22
CK	Deionized water			/	0.00	0.02	/

147 Note: K0Na1, K1Na1 and K1Na0 indicate the saline water at EC of 4 dS m⁻¹ with
 148 K^+/Na^+ of 0:1, 1:1 and 1:0, respectively; CK, deionized water; CROSS represents cation
 149 ratio of soil structural stability.

150 The experiment was implemented in the form of alternate leaching, the prolonged
 151 leaching process of soil substrates proved more useful for illuminating the function of
 152 electrolyte effect and cation exchange (Shaygan et al., 2017). The next infiltration was
 153 performed two days after the drainage of the previous infiltration was completed. Soil
 154 layers were regarded as reaching desalination prerequisite when the soil salt content
 155 came to less than 0.3%, which meant that bulk electrical conductivity was less than 1.5
 156 dS m⁻¹ (transformation from salt content to bulk electrical conductivity) (Yin et al.,
 157 2022). Water application was stopped when the bulk electrical conductivity of all
 158 treatments at 15 cm depth reached the prerequisite for desalination. This experiment
 159 was planned to fill all the pores in the soil column throughout the infiltration cycle,
 160 therefore the water applied at the first infiltration was described by the pore volume
 161 equation (Xu and Huang 2010):

$$162 \quad V_p = V_s \cdot TP \quad (2)$$



163
$$TP = \frac{ds - BD}{ds} \quad (3)$$

164 where V_p is the pore volume (cm^3), V_s is the volume of filled soil (cm^3), TP is the soil
165 total porosity (%), ds is the soil particle density (2.65 g cm^{-3}) (Xu and Huang 2010),
166 BD is the bulk density (g cm^{-3}). According to Eq. (2) and Eq. (3), around 6 L of water
167 was required in the first infiltration. Required water volume for each subsequent
168 leaching was determined by the volume of leachate at the first infiltration, 0.5 L each
169 time.

170 2.3 Measurements

171 During the whole experiment period, soil volumetric water content and bulk
172 electrical conductivity were real-time monitored at 15 and 30 cm soil depths from the
173 soil surface by capacitance sensors (ECH2O 5TE, METER Group, USA) (Fig. 1). The
174 leachate was collected in the leachate catcher below the soil column. Cumulative
175 leachate volume was monitored over time to determine the saturated hydraulic
176 conductivity (K_{sat} , cm min^{-1}) of each treatment by using a derivation of Darcy's
177 approach (Sahin et al., 2011):

178
$$K_{\text{sat}} = \frac{V_l \cdot H}{A \cdot t \cdot (H + h)} \quad (4)$$

179 where V_l is the leachate volume (cm^3), H is the length of filled soil (cm), A is the surface
180 area of soil column (cm^2), t is the leaching time of measurement (min), h is the height
181 of constant water head (cm).

182 The salt accumulated in the soil column was determined by subtracting the salt in



183 the leachate from the applied water, the salination rate (R_s , %) indicated the ratio of salt
184 accumulated in the soil column at every time of infiltration to the salt content at the first
185 applied water. Leaching efficiency (Le , $g L^{-1}$) referred to the amount of desalination per
186 unit of water volume in the desalination process. R_s and Le were calculated as follows:

187
$$R_s = m_s / m_w \quad (5)$$

188
$$Le = (m_s - m_1) / w \quad (6)$$

189 Where m_s is the salt content accumulated in soil column at every time of infiltration (g),
190 m_w is the salt content in the total water used for the first infiltration (g), m_1 is the mass
191 of salts after the first infiltration (g), w is the total water volume used for leaching (L).

192 Soil samples were collected from each soil column at 5-cm intervals with the 0-40
193 cm soil layer three days after the final infiltration. Soil BD was calculated using the soil
194 core method, and TP was calculated by Eq. (3) based on BD . Soil water characteristics
195 curve was measured with the high velocity centrifugal method (CR21 Hitachi, Japan),
196 and calibrated by RETC software (PC Progress Inc., Prague, Czech Republic).
197 Currently, several defining sizes of macropores are proposed, rather than a precise
198 definition and pore size range (Cameira et al. 2003; Kim et al. 2010; Hu et al. 2018;
199 Budhathoki et al. 2022; Aldaz-Lusarreta et al. 2022). In this study, macropores were
200 defined as the pores with diameters larger than 1 mm, whereas micropores were defined
201 as smaller than 1 mm (Luxmoore 1981; Wilson and Luxmoore 1988). Based on the
202 capillary pressure data, the relationship between pore diameter (d , mm) and water
203 suction (S , Pa) was described according to the capillary bundle model (Jury et al., 1991):



204
$$d = \frac{300}{S} \quad (7)$$

205 **2.4 Statistical analysis**

206 Statistical analysis among all treatments with different K^+/Na^+ was performed in
207 SPSS 22.0 software, using one-way analysis of variance (ANOVA) based on the least
208 significant difference (LSD) test at 95% significance level ($P < 0.05$). All figures were
209 created through Origin 2022b.

210 **3 Results**

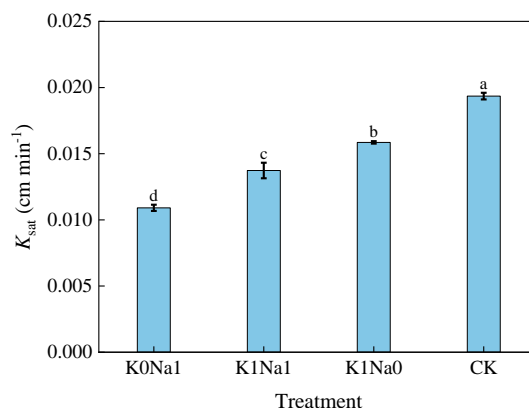
211 **3.1 Soil saturated hydraulic conductivity (K_{sat})**

212 The K0Na1, K1Na1 and K1Na0 significantly ($P < 0.05$) reduced K_{sat} by 43.62%,
213 29.04% and 18.06% compared with CK, respectively (Fig. 2). Additionally, K_{sat} was
214 negatively correlated with CROSS of saline water, increasing the CROSS of the applied
215 saline water generally reduced K_{sat} .

216

217

218

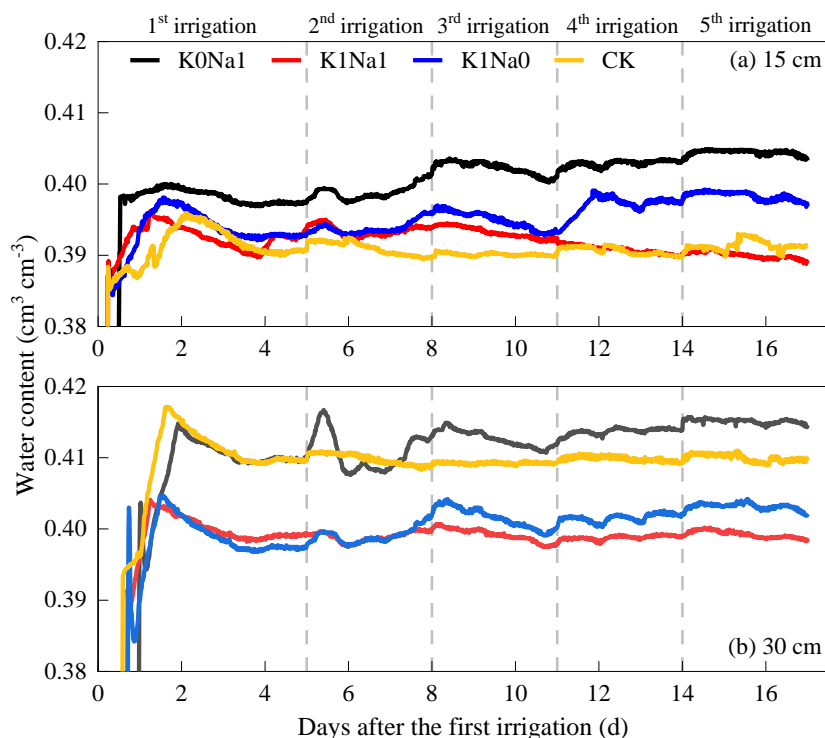


219

220 Fig. 2. Saturated hydraulic conductivity (K_{sat}) under different treatments. K0Na1,
221 K1Na1 and K1Na0 indicate the saline water at EC of 4 dS m⁻¹ with K⁺/Na⁺ of 0:1, 1:1
222 and 1:0, respectively; CK, deionized water; Different letters after means of K_{sat} indicate
223 statistical differences ($P < 0.05$) among treatments based on LSD. Bars indicate
224 standard deviations of means.

225 3.2 Soil water content

226 Water content increased immediately after each infiltration for all treatments, and
227 then gradually declined to a constant level (Fig. 3). And water content at deeper soil
228 depths was greater than at shallow soil depths at the same time during the whole
229 infiltration period. The water content ranged from 0.39-0.41 and 0.40-0.42 cm³ cm⁻³ at
230 15 and 30 cm soil depths, respectively. K0Na1 gained the highest water content at both
231 15 and 30 cm soil depths. K1Na1 and K1Na0 were greater than CK at 15 cm soil depth
232 and lower than CK at 30 cm soil depth, and the water content of K1Na1 was higher
233 than K1Na0 at both 15 and 30 cm soil layers.



234

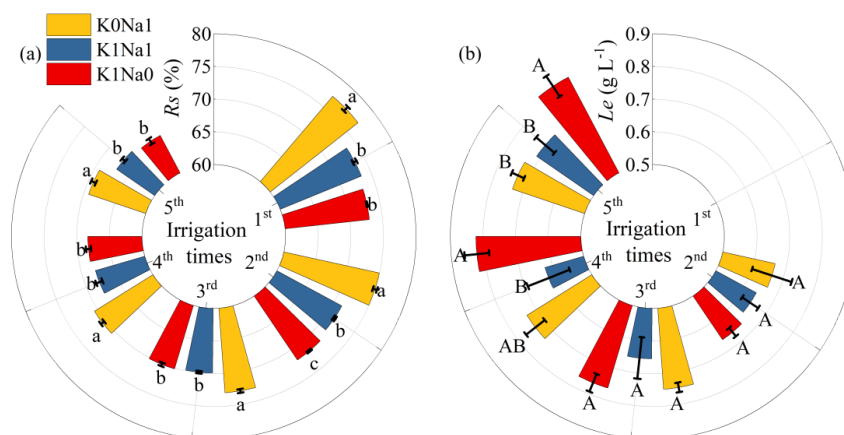
235 Fig. 3. Variation of water content over time under different treatments at 15 (a) and 30
236 cm (b) soil depths during the five times of infiltration.

237 3.3 Soil salination rate (R_s) and leaching efficiency (Le)

238 The R_s and Le under CK were not shown in Fig. 4, because deionized water was
239 used as the control and there was almost no salt contained in the study soil, CK was
240 considered negligible for salt accumulation and leaching. R_s peaked at the first
241 infiltration, and approximately 70%-80% of the salt in the saline water was retained in
242 the soil column, after which the subsequent leaching had lower R_s values (Fig. 4). The
243 lower the ratio of K^+/Na^+ , the larger soil R_s . Among the three saline water treatments,



244 K1Na0 had the lowest R_s and highest Le at five infiltrations.



245

246 Fig. 4. Salination rate (R_s) (a) and leaching efficiency (Le) (b) at five infiltrations under

247 all saline water treatments. K0Na1, K1Na1 and K1Na0 indicate the saline water at EC

248 of 4 dS m^{-1} with K^+/Na^+ of 0:1, 1:1 and 1:0, respectively; Different lowercase letters

249 followed means of R_s indicate statistical differences ($P < 0.05$) among treatments based

250 on LSD, and different capital letters followed means of Le indicate statistical

251 differences ($P < 0.05$) among treatments based on LSD. Bars indicate standard

252 deviations of means.

253 3.4 Soil bulk electrical conductivity

254 Bulk electrical conductivity of K0Na1, K1Na1 and K1Na0 ranged from 1.0 to 2.0

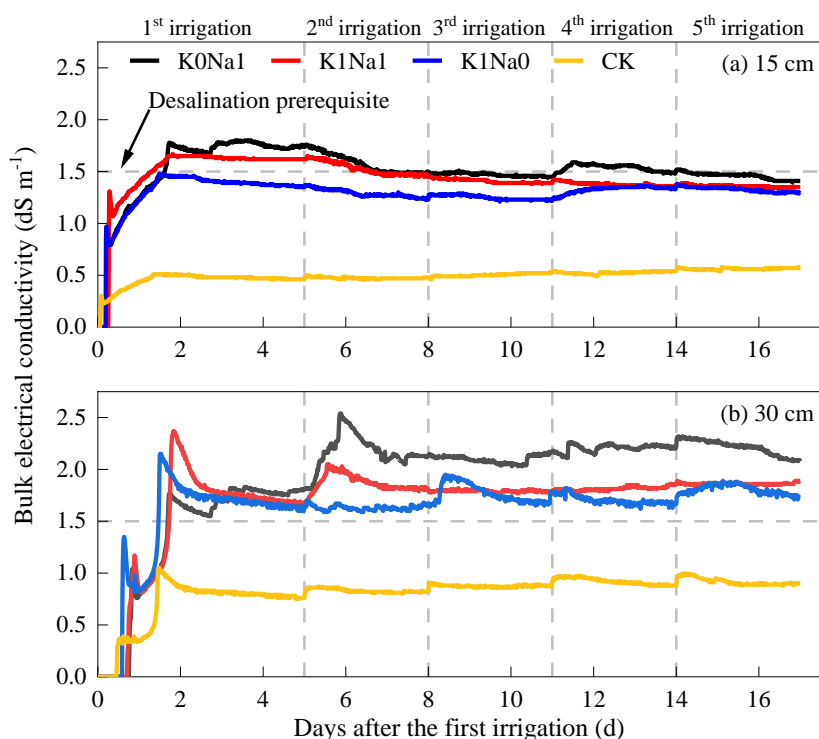
255 dS m^{-1} at 15 cm, 1.5 to 2.5 dS m^{-1} at 30 cm soil depth (Fig. 5). After the first infiltration,

256 bulk electrical conductivity in 15 cm soil layer reached its apes, and then exhibited a

257 general downward trend in the following infiltrations. However, more salts were



258 leached to deeper layers, where salt began to accumulate instead of desalination, and
259 bulk electrical conductivity at 30 cm soil depth gradually increased following the
260 infiltration events. At both 15 and 30 cm soil layers, the bulk electrical conductivity of
261 K0Na1 was considerably greater than K1Na1, and K1Na1 was quite higher than K1Na0.



262
263 Fig. 5. Variation of bulk electrical conductivity over time under treatments with
264 different K^+/Na^+ at constant EC at 15 (a) and 30 cm (b) soil depths in the period of five
265 times of infiltration. K0Na1, K1Na1 and K1Na0 indicate the saline water at EC of 4 dS
266 m^{-1} with K^+/Na^+ of 0:1, 1:1 and 1:0, respectively; CK, deionized water.

267 At 15 cm soil depth, K0Na1 reached the soil desalination prerequisite after the
268 fifth infiltration, while K1Na1 reached the desalination prerequisite after the second
269 infiltration, and K1Na0 did not exceed desalination prerequisite during the whole

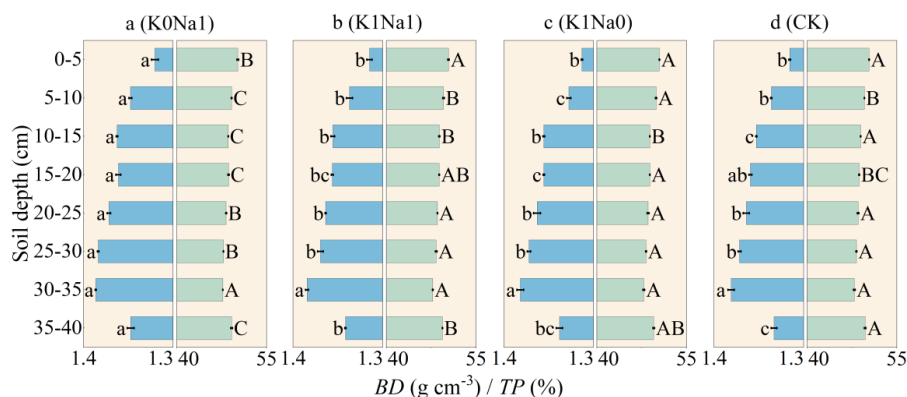


270 infiltration period. Among all saline water treatments, K1Na0 saved the desalination
271 time and required leaching volume to reach the standard of desalination. K0Na1,
272 K1Na1 and K1Na0 did not meet the desalination prerequisite at 30 cm soil depth, and
273 the increased volume of infiltration water also increased the bulk electrical conductivity.

274 **3.5 Soil bulk density (*BD*) and total porosity (*TP*)**

275 Soil *BD* varied between 1.30 and 1.40 g cm⁻³ for all treatments, and *BD* was below
276 1.35 g cm⁻³ at 0-10 and 35-40 cm soil layers, however, over 1.35 g cm⁻³ at 10-35 cm
277 soil depth (Fig. 6). K0Na1 significantly ($P < 0.05$) enhanced soil *BD* throughout the soil
278 column profile compared with CK. *TP* first diminished with soil depth to reach a
279 minimum at about 30-35 cm, and then slightly increased at 35-40 cm. The *TP* of K1Na1
280 and K1Na0 slightly improved after five times of infiltration, and only K0Na1 showed
281 a decline compared with CK. Overall, over the whole infiltration period, K1Na0 was
282 most conducive to the formation of soil pore structure and increasing the total pore
283 volume. The saline water with lower CROSS was beneficial for reducing soil *BD* and
284 increasing *TP*.

285



286

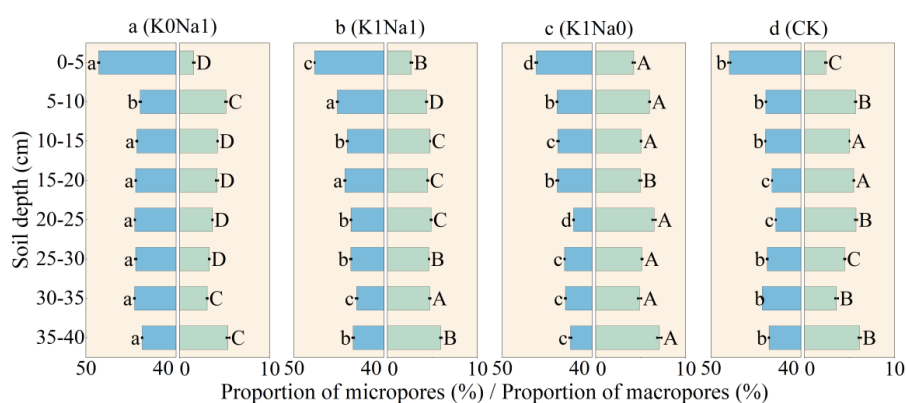
287 Fig. 6. Soil bulk density (*BD*) and total porosity (*TP*) throughout the soil column profile
 288 under different treatments. K0Na1, K1Na1 and K1Na0 indicate the saline water at EC
 289 of 4 dS m⁻¹ with K⁺/Na⁺ of 0:1, 1:1 and 1:0, respectively; CK, deionized water; The
 290 blue horizon columns represent *BD*, while the green horizon columns represent *TP*;
 291 Different lowercase letters followed means of *BD* indicate statistical differences ($P <$
 292 0.05) among treatments based on LSD, and different capital letters followed means of
 293 *TP* indicate statistical differences ($P < 0.05$) among treatments based on LSD. Bars
 294 indicate standard deviations of means.

295 3.6 Proportion of micropores and proportion of macropores

296 Micropores were the dominant pores for all treatments, the proportion of
 297 micropores accounting for more than 40% of the total soil volume, however, the
 298 proportion of macropores made up no more than 8% (Fig. 7). 0-5 cm soil layer had the
 299 lowest proportion of macropores and retained the largest proportion of micropores
 300 compared with other depths. K0Na1 had the highest proportion of micropores and the



301 lowest proportion of macropores. K1Na0 had a greater proportion of macropores in the
 302 soil column compared with CK.



303

304 Fig. 7. Proportion of micropores and proportion of macropores in total soil volume
 305 throughout the soil column profile under different treatments. K0Na1, K1Na1 and
 306 K1Na0 indicate the saline water at EC of 4 dS m⁻¹ with K⁺/Na⁺ of 0:1, 1:1 and 1:0,
 307 respectively; CK, deionized water; The blue horizon columns represent proportion of
 308 micropores, while the green horizon columns represent proportion of macropores;
 309 Different lowercase letters followed means of proportion of micropores indicate
 310 statistical differences (P < 0.05) among treatments based on LSD, and different capital
 311 letters followed means of proportion of macropores indicate statistical differences (P <
 312 0.05) among treatments based on LSD. Bars indicate standard deviations of means.

313 **4 Discussion**

314 **4.1 Effects of saline water on soil water movement and redistribution**

315 As a crucial soil hydraulic characteristic, K_{sat} represents the transportation ability



316 of water and solutes (Braud et al. 2001; Maillard et al. 2011; Albalasmeh et al. 2022).
317 The cation composition and EC of soil solution affect K_{sat} by controlling electrostatic
318 repulsive pressure through surface potential and midpoint potential between adjacent
319 particles, and consequently influence water movement (Fares et al. 2000; Liu et al.,
320 2022b). Specifically, the K^+/Na^+ ratio in saline water was related to the swelling and
321 dispersion of soil particles (Yu et al. 2016; Zhu et al. 2019). Dispersed clay particles
322 clogged soil macropores to subsequently restrict water transport (Awedat et al., 2021).
323 The Na^+ has a relatively higher ionicity index than K^+ , as a result, the low K^+/Na^+ ratio
324 decreased the degree of covalency in clay-cation bonds, which was detrimental to clay
325 particles aggregation (Marchuk and Rengasamy 2011). Therefore, in our study, the high
326 K^+/Na^+ ratio promoted the flocculation and stabilization of soil clay particles, resulting
327 in an increased infiltration rate.

328 After a certain period of water supply, soil moisture redistributed at different
329 depths of soil column. Soil water moved further down during the phase of water
330 redistribution soon after each irrigation, reducing the water content in the upper soil
331 layers. As the upper soil layers drained, the lower soil layers still had water inflow
332 (Kargas et al., 2021), increasing the water content in the lower soil layers. The results
333 also implicated that the retention of soil water by Na^+ was stronger than that by K^+ , the
334 cause may be that Na^+ can increase the thickness of the diffuse-double layers around
335 soil colloids theoretically due to its larger hydrated radius and lower charge than K^+ ,
336 and the adjacent double layers overlapped to provide more space between layers, where,



337 subsequently, more water can be retained (He et al., 2015). Additionally, our study
338 showed that an appropriate concentration of K^+/Na^+ was even more beneficial than
339 deionized water for water downward transport, which could be because the deionized
340 water (CK) (below 0.2 dS m^{-1}) tended to leach soluble minerals and salts, especially
341 Ca^{2+} , from the surface soil layers. This would lead to the reduction of its original solid
342 soil structural stability. In the absence of salt and Ca^{2+} , the dispersed tiny particles filled
343 the smaller pore spaces in soil, reducing even more channels for water flow and
344 exacerbating water retention in deeper soil layers (Ayers and Westcot 1985). However,
345 a lower concentration of soluble salts could increase colloid flocculation, and thereby,
346 improve soil aeration and water conductivity (Tang and She 2016).

347 **4.2 Effects of saline water on soil salination and desalination process**

348 Numerous factors influence the leaching efficiency of soil salts; for example,
349 increasing EC and reducing SAR definitely improve clay flocculation, which can
350 enhance salt leaching (Ebrahim Yahya et al., 2022). Na^+ is more likely to trigger soil
351 clay dispersion and swelling than K^+ , thus Na^+ generally inhibits water infiltration,
352 which is detrimental to salt leaching (Smiles and Smith 2004). Adding K^+ could
353 promote displacement of the adsorbed Na^+ , and then decrease Na^+ concentration and
354 salt accumulation in soil solute through leaching.

355 A greater reduction in Na^+ concentration was associated with a higher rate of
356 cation exchange rate, and the slow rate of solute leaching from aggregates reduced the



357 total leaching efficiency (Shaygan et al., 2017). During the leaching process, water flow
358 preferentially passed through the macropores rather than aggregates. The slow water
359 transportation through aggregates induced the slow removal of solutes from the
360 aggregates, leading to a reduced leaching efficiency. In our study, the alternate leaching
361 was implemented to improve solute leaching. The soil solutes diffused into the
362 aggregates surface during the rest period, improving salt leaching due to the water flow
363 in macropores (Al-Sibai et al., 1997). Increasing K^+/Na^+ ratio could increase the
364 magnitude of cation exchange due to the substitution of Na^+ on exchange sites by K^+
365 with lower dispersive potential (Shaygan et al., 2017), the intensive release of cations
366 from the soil further improved salt's leaching efficiency. In addition, the integrity of
367 soil aggregates created by combining clay particles and the other soil components
368 enhanced by K^+ can benefit solute transportation (Marchuk and Rengasamy 2011).

369 **4.3 Effects of saline water on soil pore structure characteristics**

370 The upper soil was longer exposed to water due to the long-term continuous
371 irrigation, causing the particles to swell and the surface layer to loosen (Vaezi et al.
372 2017; Håkansson and Lipiec 2000), and also the decreased BD in the surface layer of
373 soil column. The subsoil BD increased with depth under the impact of water pressure
374 and self-weight due to the declining pore diameter and pore branching closure
375 (Schjønning et al., 2013). And for soil at the bottom, the loss of soil particles from small
376 holes was responsible for the abrupt reduction in BD . The value of CROSS in saline



377 water could reflect changes in soil *BD* and *TP*, in agreement with the result of Marchuk
378 and Marchuk (2018). The high CROSS implied an increase in the proportion of
379 monovalent exchangeable cations, thickening the double layer at the interface between
380 the clay surface and soil solution. Hence, soil swelling occurred at the expense of water-
381 conducting pores. Additionally, aggregates slaking and subsequent clay dispersion and
382 deposition of clay particles within the pore space contributed to the reduction in *TP*
383 (Marchuk and Marchuk 2018).

384 Fewer soil macropores plays a crucial role in water and solute transport,
385 accounting for 85% of the total infiltration volume (Wilson and Luxmoore 1988; Weiler
386 and Naef 2003; Kotlar et al. 2020). The lower the K^+/Na^+ ratio, the more it enhanced
387 soil clay dispersion, resulting in the loosening of clay particles from the aggregates.
388 This, in turn, dispersed clay particles moved with water caused the macropores to
389 become blocked, converting them into micropores (Cameira et al., 2003), thus leading
390 to a decrease in the volume of soil macropores.

391 **5 Conclusion**

392 We explored the effect of K^+/Na^+ in saline water on soil hydraulic characteristics
393 and structural stability via a soil column experiment. The higher K^+/Na^+ ratio caused
394 fewer pore blockages due to soil clay particle dispersion than lower K^+/Na^+ , which
395 increased soil saturated hydraulic conductivity. The presence of K^+ accelerated the
396 sustained Na^+ replacement and leaching, alleviating salt accumulation and enhancing



397 leaching efficiency. Increasing K^+/Na^+ positively affected the establishment of soil
398 structure due to the transformation of micropores into macropores, and the ever-
399 increasing unobstructed water-conducting channels sped up water and solute transport.
400 The rational use of saline water with adequate K^+ could help mitigate the structural
401 deterioration caused by Na^+ . Appropriate adjustment of saline water K^+/Na^+ during
402 infiltration could ameliorate soil structural properties. In addition to Ca^{2+} and Mg^{2+}
403 (primary concerns in earlier studies), the relative concentration of K^+ to Na^+ is an
404 essential indicator for assessing the suitability of saline water quality for irrigation and
405 should be considered when using saline water.

406 **Author contributions**

407 Sihui Yan and Tabin Zhang conceived and designed the experiments. Sihui Yan,
408 Binbin Zhang and Tonggang Zhang led the data processing and statistical analysis,
409 Sihui Yan, Yu Cheng, Chun Wang and Min Luo performed the experiments. Sihui Yan
410 wrote the initial draft. Hao Feng and Kadambot H.M. Siddique contributed to review
411 and editing of the paper.

412 **Acknowledgments**

413 This work was supported by the National Key R&D Program of China (Grant No.
414 2021YFD1900700) and National Natural Science Foundation of China (Grant No.
415 51879224, 51509238).



416 **References**

- 417 Albalasmeh, A., Mohawesh, O., Gharaibeh, M., Deb, S., Slaughter, L., El Hanandeh, A.: Artificial
418 neural network optimization to predict saturated hydraulic conductivity in arid and semi-arid
419 regions, *Catena*, 217, 106459, <https://doi.org/10.1016/j.catena.2022.106459>, 2022.
- 420 Aldaz-Lusarreta, A., Giménez, R., Campo-Bescós, M.A., Arregui, L.M., Virto, I.: Effects of
421 innovative long-term soil and crop management on topsoil properties of a Mediterranean soil
422 based on detailed water retention curves, *SOIL*, 8, 655-671, [https://doi.org/10.5194/egusphere-](https://doi.org/10.5194/egusphere-2022-1092)
423 [2022-1092](https://doi.org/10.5194/egusphere-2022-1092), 2022, 2022.
- 424 Al-Sibai, M., Adey, M.A., Rose, D.A.: Movement of solute through a porous medium under
425 intermittent leaching, *Eur. J. Soil Sci.*, 48, 711-725, [https://doi.org/10.1046/j.1365-](https://doi.org/10.1046/j.1365-2389.1997.00126.x)
426 [2389.1997.00126.x](https://doi.org/10.1046/j.1365-2389.1997.00126.x), 1997.
- 427 Alva, A.K., Sumner, M.E., Miller, W.P.: Relationship between ionic strength and electrical
428 conductivity for soil solutions, *Soil Sci.*, 152, 239-242, [https://doi.org/10.1097/00010694-](https://doi.org/10.1097/00010694-199110000-00001)
429 [199110000-00001](https://doi.org/10.1097/00010694-199110000-00001), 1991.
- 430 Aparicio, J., Tenza-Abril, A.J., Borg, M., Galea, J., Candela, L.: Agricultural irrigation of vine crops
431 from desalinated and brackish groundwater under an economic perspective. A case study in
432 Siggiewi, Malta, *Sci. Total Environ.*, 650, 734-740,
433 <https://doi.org/10.1016/j.scitotenv.2018.09.059>, 2019.
- 434 Awedat, A.M., Zhu, Y., Bennett, J.M., Raine, S.R.: The impact of clay dispersion and migration on
435 soil hydraulic conductivity and pore networks, *Geoderma*, 404, 115297,
436 <https://doi.org/10.1016/j.geoderma.2021.115297>, 2021.



- 437 Ayers, R.S., Westcot, D.W.: Water Quality for Agriculture, FAO Irrigation and Drainage Paper 29
438 Rev 1, Rome, Italy.
- 439 Bao, S.D.: Soil Analysis in Agricultural Chemistry, China Agricultural Press, Beijing, China, 2005
440 (in Chinese).
- 441 Belkheiri, O., Mulas, M.: The effects of salt stress on growth, water relations and ion accumulation
442 in two halophyte *Atriplex* species, *Environ. Exp. Bot.*, 86, 17-28,
443 <https://doi.org/10.1016/j.envexpbot.2011.07.001>, 2013.
- 444 Bouksila, F., Bahri, A., Berndtsson, R., Persson, M., Rozema, J., Van der Zee, S.E.A.T.M.:
445 Assessment of soil salinization risks under irrigation with brackish water in semiarid Tunisia,
446 *Environ. Exp. Bot.*, 92, 176-185, <https://doi.org/10.1016/j.envexpbot.2012.06.002>, 2013.
- 447 Braud, I., Vich, A.I.J., Zuluaga, J., Fornero, L., Pedrani, A.: Vegetation influence on runoff and
448 sediment yield in the Andes region: observation and modelling, *J. Hydrol.*, 254, 124-144,
449 [https://doi.org/10.1016/S0022-1694\(01\)00500-5](https://doi.org/10.1016/S0022-1694(01)00500-5), 2001.
- 450 Budhathoki, S., Lamba, J., Srivastava, P., Malhotra, K., Way, T.R., Katuwal, S.: Using X-ray
451 computed tomography to quantify variability in soil macropore characteristics in pastures, *Soil
452 Tillage Res.*, 215, 105194, <https://doi.org/10.1016/j.still.2021.105194>, 2022.
- 453 Buelow, M.C., Steenwerth, K., Parikh, S.J.: The effect of mineral-ion interactions on soil hydraulic
454 conductivity, *Agric. Water. Manag.*, 152, 277-285, <https://doi.org/10.1016/j.agwat.2015.01.015>,
455 2015.
- 456 Cameira, M.R., Fernando, R.M., Pereira, L.S.: Soil macropore dynamics affected by tillage and
457 irrigation for a silty loam alluvial soil in southern Portugal, *Soil Tillage Res.*, 70, 131-140,



- 458 [https://doi.org/10.1016/S0167-1987\(02\)00154-X](https://doi.org/10.1016/S0167-1987(02)00154-X), 2003.
- 459 Ebrahim Yahya, K., Jia, Z., Luo, W., Yuanchun, H., Ame, M.A.: Enhancing salt leaching efficiency
460 of saline-sodic coastal soil by rice straw and gypsum amendments in Jiangsu coastal area, Ain
461 Shams Eng. J., 13, 101721, <https://doi.org/10.1016/j.asej.2022.101721>, 2022.
- 462 Fares, A., Alva, A.K., Nkedi-Kizza, P., Elrashidi, M.A.: Estimation of soil hydraulic properties of a
463 sandy soil using capacitance probes and Guelph Permeameter, Soil Sci. Soc. Am. J., 165, 768-
464 777, <https://doi.org/10.1097/00010694-200010000-00002>, 2000.
- 465 Gharaibeh, M.A., Eltaif, N.I., Shunnar, O.F.: Leaching and reclamation of calcareous saline-sodic
466 soil by moderately saline and moderate-SAR water using gypsum and calcium chloride, J. Plant
467 Nutr. Soil Sci., i.-Z. Pflanzenernahr. Bodenkd., 172, 713–719,
468 <http://dx.doi.org/10.1002/jpln.200700327>, 2009.
- 469 Hack-Ten Broeke, M.J.D., Kroes, J.G., Bartholomeus, R.P., Van Dam, J.C., De Wit, A.J.W., Supit,
470 I., Walvoort, D.J.J., Van Bakel, P.J.T., Ruijtenberg, R.: Quantification of the impact of
471 hydrology on agricultural production as a result of too dry, too wet or too saline conditions,
472 SOIL, 2, 391-402, <https://doi.org/10.5194/soil-2-391-2016>, 2016.
- 473 Håkansson, I., Lipiec, J.: A review of the usefulness of relative bulk density values in studies of soil
474 structure and compaction, Soil Tillage Res., 53, 71-85, [https://doi.org/10.1016/S0167-1987\(99\)00095-1](https://doi.org/10.1016/S0167-1987(99)00095-1), 2000.
- 476 He, Y.B., Desutter, T.M., Casey, F., Clay, D., Franzen, D., Steele, D.: Field capacity water as
477 influenced by Na and EC: Implications for subsurface drainage, Geoderma, 245, 83-88,
478 <https://doi.org/10.1016/j.geoderma.2015.01.020>, 2015.



- 479 Hu, X., Li, Z.C., Li, X.Y., Wang, P., Zhao, Y.D., Liu, L.Y., LÜ, Y.L.: Soil macropore structure
480 characterized by X-Ray computed tomography under different land uses in the Qinghai Lake
481 watershed, Qinghai-Tibet plateau., *Pedosphere*, 28, 478-487, [https://doi.org/10.1016/S1002-](https://doi.org/10.1016/S1002-0160(17)60334-5)
482 0160(17)60334-5, 2018.
- 483 Jury, W., Gardner, W.R., Gardner, W.H.: *Soil Physics*, John Wiley and Sons, New York, USA, 1991.
- 484 Kargas, G., Soulis, K.X., Kerkides, P.: Implications of hysteresis on the horizontal soil water
485 redistribution after infiltration, *Water*, 13, 2773-2773, <https://doi.org/10.3390/W13192773>,
486 2021.
- 487 Kim, H., Anderson, S.H., Motavalli, P.P., Gantzer, C.J.: Compaction effects on soil macropore
488 geometry and related parameters for an arable field, *Geoderma*, 160, 244-251,
489 <https://doi.org/10.1016/j.geoderma.2010.09.030>, 2010.
- 490 Kotlar, A.M., de Jong van der Lier, Q., Andersen, H.E., Nørgaard, T., Iversen, B.V.: Quantification of
491 macropore flow in Danish soils using near-saturated hydraulic properties, *Geoderma*, 375,
492 114479, <https://doi.org/10.1016/j.geoderma.2020.114479>, 2020.
- 493 Li, Z.Y., Cao, W.G., Wang, Z.R., Li, J.C., Ren, Y.: Hydrochemical characterization and irrigation
494 suitability analysis of shallow groundwater in Hetao Irrigation District, Inner Mongolia.,
495 *Geoscience*, 36, 418-426, <https://doi.org/10.19657/j.geoscience.1000-8527.2022.012>, 2022 (in
496 Chinese).
- 497 Liu, B.X., Wang, S.Q., Liu, X.J., Sun, H.Y.: Evaluating soil water and salt transport in response to
498 varied rainfall events and hydrological years under brackish water irrigation in the North China
499 Plain, *Geoderma*, 422, 115954, <https://doi.org/10.1016/j.geoderma.2022.115954>, 2022a.



- 500 Liu, X.M., Zhu, Y.C., Mclean Bennett, J., Wu, L.S., Li, H.: Effects of sodium adsorption ratio and
501 electrolyte concentration on soil saturated hydraulic conductivity, *Geoderma*, 414, 115772,
502 <https://doi.org/10.1016/j.geoderma.2022.115772>, 2022b.
- 503 Luxmoore, R.J.: Micro-, meso-, and macroporosity of soils., *Soil Sci. Soc. Am. J.*, 45, 671-672,
504 <https://doi.org/10.2136/sssaj1981.03615995004500030051x>, 1981.
- 505 Maillard, E., Payraudeau, S., Faivre, E., Grégoire, C., Gangloff, S., Imfeld, G.: Removal of pesticide
506 mixtures in a stormwater wetland collecting runoff from a vineyard catchment, *Sci. Total*
507 *Environ.*, 409, 2317-2324, <https://doi.org/10.1016/j.scitotenv.2011.01.057>, 2011.
- 508 Marchuk, A., Marchuk, S.A., Bennett, J.A., Eyres, M.A., Scott, E.: An alternative index to ESP to
509 explain dispersion occurring in Australian soils when Na content is low, *National Soils*
510 *Conference: Proceedings of the 2014 National Soils Conference Soil Science Australia*
511 *Melbourne, Australia, 2014.*
- 512 Marchuk, A., Rengasamy, P.: Clay behaviour in suspension is related to the ionicity of clay-cation
513 bonds, *Appl. Clay Sci.*, 53, 754-759, <https://doi.org/10.1016/j.clay.2011.05.019>, 2011.
- 514 Marchuk, S., Marchuk, A.: Effect of applied potassium concentration on clay dispersion, hydraulic
515 conductivity, pore structure and mineralogy of two contrasting Australian soils., *Soil Tillage*
516 *Res.*, 182, 35-44, <https://doi.org/10.1016/j.still.2018.04.016>, 2018.
- 517 Mckenna, B.A., Kopittke, P.M., Macfarlane, D.C., Dalzell, S.A., Menzies, N.W.: Changes in soil
518 chemistry after the application of gypsum and sulfur and irrigation with coal seam water,
519 *Geoderma*, 337, 782-791, <https://doi.org/10.1016/j.geoderma.2018.10.019>, 2019.
- 520 Prajapati, M., Shah, M., Soni, B.: A review of geothermal integrated desalination: A sustainable



- 521 solution to overcome potential freshwater shortages, *J. Clean. Prod.*, 326, 129412,
522 <https://doi.org/10.1016/j.jclepro.2021.129412>, 2021.
- 523 Qadir, M., Oster, J.D., Schubert, S., Noble, A.D., Sahrawat, K.L.: Phytoremediation of Sodic and
524 Saline-Sodic Soils, *Adv. Agron.*, 96, 197-247, [https://doi.org/10.1016/S0065-2113\(07\)96006-](https://doi.org/10.1016/S0065-2113(07)96006-X)
525 X, 2007.
- 526 Qadir, M., Sposito, G., Smith, C.J., Oster, J.D.: Reassessing irrigation water quality guidelines for
527 sodicity hazard, *Agric. Water. Manag.*, 255, 107054,
528 <https://doi.org/10.1016/j.agwat.2021.107054>, 2021.
- 529 Reading, L.P., Lockington, D.A., Bristow, K.L., Baumgartl, T.: Are we getting accurate
530 measurements of Ksat for sodic clay soils? *Agric. Water. Manag.*, 158, 120-125,
531 <https://doi.org/10.1016/j.agwat.2015.04.015>, 2015.
- 532 Rengasamy, P., Marchuk, A.: Cation ratio of soil structural stability (CROSS), *Soil Res.*, 49, 280-
533 285, <https://doi.org/10.1071/SR10105>, 2011.
- 534 Sahin, U., Eroğlu, S., Sahin, F.: Microbial application with gypsum increases the saturated hydraulic
535 conductivity of saline-sodic soils, *Appl. Soil Ecol.*, 48, 247-250,
536 <https://doi.org/10.1016/j.apsoil.2011.04.001>, 2011.
- 537 Schjønning, P., Lamandé, M., Berisso, F.E., Simojoki, A., Alakukku, L., Andreasen, R.R.: Gas
538 diffusion, non-darcy air permeability, and computed tomography images of a clay subsoil
539 affected by compaction, *Soil Sci. Soc. Am. J.*, 77, 1977-1990,
540 <https://doi.org/10.2136/sssaj2013.06.0224>, 2013.
- 541 Scudiero, E., Skaggs, T.H., Corwin, D.L.: Simplifying field-scale assessment of spatiotemporal



542 changes of soil salinity, *Sci. Total Environ.*, 587-588, 273-281,
543 <https://doi.org/10.1016/j.scitotenv.2017.02.136>, 2017.

544 Shaygan, M., Reading, L.P., Baumgartl, T.: Effect of physical amendments on salt leaching
545 characteristics for reclamation, *Geoderma*, 292, 96-110,
546 <https://doi.org/10.1016/j.geoderma.2017.01.007>, 2017.

547 Singh, G., Mavi, M.S., Choudhary, O.P., Gupta, N., Singh, Y.: Rice straw biochar application to soil
548 irrigated with saline water in a cotton-wheat system improves crop performance and soil
549 functionality in north-west India, *J. Environ. Manage.*, 295, 113277,
550 <https://doi.org/10.1016/j.jenvman.2021.113277>, 2021.

551 Smiles, D.E., Smith, C.J.: A survey of the cation content of piggery effluents and some consequences
552 of their use to irrigate soils, *Soil Res.*, 42, 231-246, <https://doi.org/10.1071/SR03059>, 2004.

553 Smith, C.J., Oster, J.D., Sposito, G.: Potassium and magnesium in irrigation water quality assessment,
554 *Agric. Water. Manag.*, 157, 59-64, <https://doi.org/10.1016/j.agwat.2014.09.003>, 2015.

555 Sposito, G., Oster, J.D., Smith, C.J., Assouline, S.: Assessing soil permeability impacts from
556 irrigation with marginal-quality waters, *AB Reviews: Perspectives in Agriculture, Veterinary
557 Science, Nutrition and Natural Resources.* 11, 15,
558 <https://doi.org/10.1079/PAVSNNR201611015>, 2016.

559 Tang, S.Q., She, D.L.: Influence of water quality on soil saturated hydraulic conductivity and
560 infiltration properties, *Transactions of the Chinese Society for Agricultural Machinery*, 47, 108-
561 114, <https://doi.org/10.6041/j.issn.1000-1298.2016.10.015>, 2016 (in Chinese).

562 Tsai, W.T., Liu, S.C., Chen, H.R., Chang, Y.M., Tsai, Y.L.: Textural and chemical properties of



- 563 swine-manure-derived biochar pertinent to its potential use as a soil amendment, *Chemosphere*,
- 564 89, 198-203, <https://doi.org/10.1016/j.chemosphere.2012.05.085>, 2012.
- 565 Vaezi, A.R., Ahmadi, M., Cerdà, A.: Contribution of raindrop impact to the change of soil physical
- 566 properties and water erosion under semi-arid rainfalls, *Sci. Total Environ.*, 583, 382-392,
- 567 <https://doi.org/10.1016/j.scitotenv.2017.01.078>, 2017.
- 568 Weiler, M., Naef, F.: Simulating surface and subsurface initiation of macropore flow, *J. Hydrol.*,
- 569 273, 139-154, [https://doi.org/10.1016/S0022-1694\(02\)00361-X](https://doi.org/10.1016/S0022-1694(02)00361-X), 2003.
- 570 Wilson, G.V., Luxmoore, R.J.: Infiltration, macroporosity, and mesoporosity distributions on two
- 571 forested watersheds, *Soil Sci. Soc. Am. J.*, 52, 329-335,
- 572 <https://doi.org/10.2136/sssaj1988.03615995005200020005x>, 1988.
- 573 Xu, J., Huang, P.M.: *Soil Science*, China Agriculture Press, Beijing, China, 2010 (in Chinese).
- 574 Yang, G., Li, F., Tian, L., He, X., Gao, Y., Wang, Z., Ren, F.: Soil physicochemical properties and
- 575 cotton (*Gossypium hirsutum* L.) yield under brackish water mulched drip irrigation, *Soil*
- 576 *Tillage Res.*, 199, 104592, <https://doi.org/10.1016/j.still.2020.104592>, 2020.
- 577 Yin, C.Y., Zhao, J., Chen, X.B., Li, L.J., Liu, H., Hu, Q.L.: Desalination characteristics and
- 578 efficiency of high saline soil leached by brackish water and Yellow River water, *Agric. Water*
- 579 *Manag.*, 263, 107461, <https://doi.org/10.1016/j.agwat.2022.107461>, 2022.
- 580 Yu, Z.H., Liu, X.M., Xu, C.Y., Xiong, H.L., Li, H.: Specific ion effects on soil water movement,
- 581 *Soil Tillage Res.*, 161, 63-70, <https://doi.org/10.1016/j.still.2016.03.004>, 2016.
- 582 Zhang, H.X., Xie, Y.Z.: Alleviating freshwater shortages with combined desert-based large-scale
- 583 renewable energy and coastal desalination plants supported by Global Energy Interconnection,



- 584 Glob. Energy Interconnec., 2, 205-213, <https://doi.org/10.1016/j.gloei.2019.07.013>, 2019.
- 585 Zhang, T.B., Zhan, X.Y., He, J.Q., Feng, H., Kang, Y.H.: Salt characteristics and soluble cations
586 redistribution in an impermeable calcareous saline-sodic soil reclaimed with an improved drip
587 irrigation, *Agric. Water. Manag.*, 197, 91-99, <https://doi.org/10.1016/j.agwat.2017.11.020>,
588 2018.
- 589 Zhu, Y., Bennett, J.M., Marchuk, A.: Reduction of hydraulic conductivity and loss of organic carbon
590 in non-dispersive soils of different clay mineralogy is related to magnesium induced
591 disaggregation, *Geoderma*, 349, 1-10, <https://doi.org/10.1016/j.geoderma.2019.04.019>, 2019.